

Fracture Toughness of PC/PBT Blend Based on J -Integral Methods

MING-LUEN LU and FENG-CHIH CHANG*

Institute of Applied Chemistry, National Chiao Tung University, Hsin-Chu, Taiwan, Republic of China

SYNOPSIS

The fracture toughness of a polycarbonate/poly(butylene terephthalate) (PC/PBT) blend was determined using three different J -integral methods, ASTM E813-81, E813-87, and hysteresis energy. The critical J values (J_{1c}) obtained are largely independent of the cross-head speed (range from 0.5 to 50 mm/min). ASTM E813-81 and hysteresis energy methods result in comparable J_{1c} values, while the E813-87 method estimates J_{1c} to be 60–80% higher. The critical displacement determined from the plots of hysteresis (energy and ratio) and the true crack growth length vs. displacement is very close. This indicates that the critical displacement determined by the hysteresis energy method is indeed the displacement at the onset of crack initiation and the corresponding J_{1c} represents a physical event of crack initiation. © 1995 John Wiley & Sons, Inc.

INTRODUCTION

By using the linear elastic fracture mechanics (LEFM) approach, the critical stress intensity factor K_{1c} ¹ is used to characterize the fracture behavior of brittle and rigid materials. However, for most low-to-moderate strength structure materials, the K_{1c} is impractical to measure. For ductile polymeric materials, such as the rubber-modified PC/PBT blends, extensive plasticity at the crack tip precludes the application of LEFM. These shortcomings from the LEFM approach induce the effort to seek other techniques that are suitable for the materials with extensive plastic yielding.

The effort has focused on the J -integral method which was originally proposed by Rice² as a means of characterizing the stress-strain singularity at a crack tip in an elastic or elastic-plastic material. Begley and Landes^{3,4} applied the J -integral concept and developed a measurement of the fracture toughness, J_{1c} , which represents the energy required to initiate crack growth. During the last decade, the J -integral approach has been applied successfully to

quantify the fracture toughness of numerous ductile polymeric materials.^{5–19} The two methods for J_{1c} determination are the multiple-specimen method developed by Begley and Landes³ or the single-specimen method developed by Rice et al.²⁰

A critical value of the J -integral, J_{1c} , has been commonly used to characterize ductile fracture in materials exhibiting large-scale yielding.^{21,22} Two key ASTM standards, E813-81 and E813-87, were established for J -testing mainly for metallic materials^{23,24} and also were extended to characterize the toughened polymers and blends during the last decade.^{5–18} However, the optimum procedures of the test have not yet been conclusively defined and standardized for polymeric materials. Subsequently, several approaches for J -integral testing have been developed. Seidler and Grellmann²⁵ studied the fracture behavior and morphologies of PC/ABS blends using a special technique: a stop block method. Mai et al.^{26–28} used the essential work method to characterize the fracture toughness for many tough polymers. Chung and Williams²⁹ used the elastic compliance method to calculate the crack growth on a three-point bending single-specimen on poly(vinylidene difluoride).

A series of hysteresis loops during load-unloading cycles were observed, which indicate the viscoelastic

* To whom correspondence should be addressed.

Table I The Tensile Test Data of PC/PBT at Different Rates

	Rate (mm/min)						
	0.5	2	5	10	20	30	50
σ_y (MPa)	44.63	46.52	46.69	47.46	49.94	50.92	52.41
E (MPa)	1839	1914	2175	2265	2451	2795	3063

σ_y : yield strength; E : Young's modulus.

and/or inelastic nature of the polymer. The accurate measurement of the crack extension by this elastic compliance method is difficult to achieve; therefore, it is rather questionable that this elastic compliance method is a reliable technique for constructing the J - R curve in the single-specimen method. In fact, when a precrack specimen of a toughened polymer is under load, viscoelastic and inelastic micromechanisms such as crazes, cavitations, debonding, and shear yielding may occur significantly around the crack-tip region. A significant fraction of the energy embodied in J is dissipated viscoelastically or inelastically before the crack extension. Therefore, it would be desirable to develop an improved hysteresis energy method to characterize the fracture toughness of the ductile polymeric materials.

In our recent studies on the fracture toughness of the elastomer-toughened polycarbonate,^{30,31} acrylonitrile-butadiene-styrene (ABS),³² high-impact polystyrene (HIPS),³³ and polycarbonate/acryloni-

trile-butadiene-styrene (PC/ABS),^{34,35} a steep rising of hysteresis under constant displacement-controlled loading was found to be related to the onset of crack initiation. An improved approach on J -integral testing based on the above-mentioned hysteresis properties has been established.³⁰⁻³⁵

CHARACTERIZING PARAMETERS OF FRACTURE MECHANICS

The J -Integral

Rice² developed the path-independent energy line integral, the J -integral, which is an energy-based parameter to characterize the stress-strain field near a crack tip surrounded by small-scale yielding. The J -integral is defined by following equation:

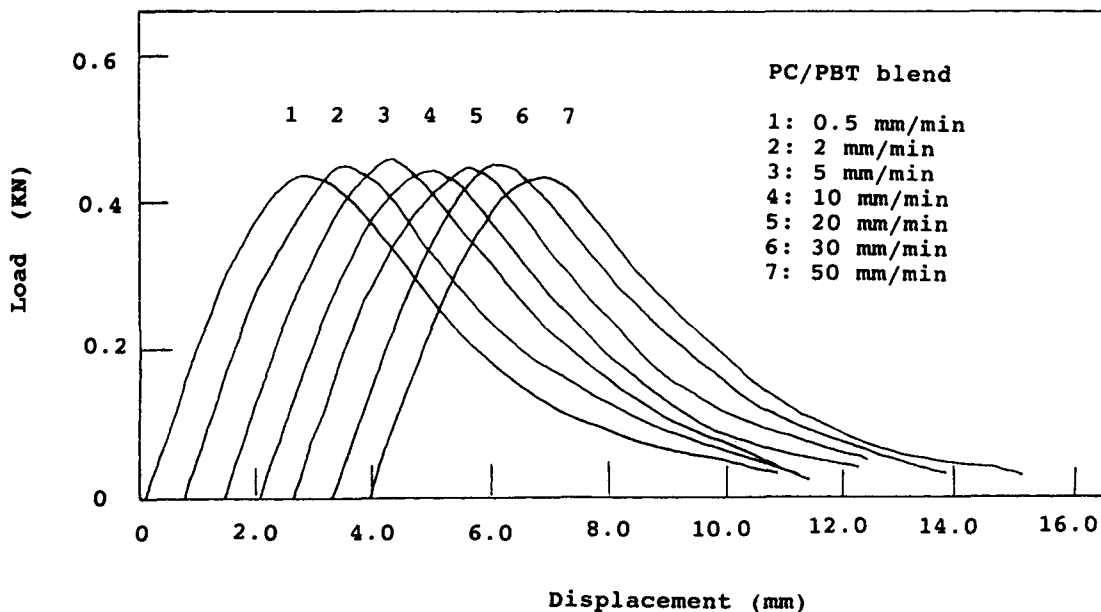


Figure 1 Plots of load displacement as a function of displacement rate.

Table II The Typical Data of the PC/PBT Blend at Rate = 2 mm/Min

<i>D</i> (mm)	Input Energy (J)	<i>J</i> (kJ/m ²)	Hysteresis Ratio (%)	Hysteresis Energy (J)	Δa (mm)
0.8	0.072	2.40	2.50	0.0018	—
1.0	0.109	3.62	2.02	0.0022	0.04
1.2	0.140	4.67	3.02	0.0042	0.08
1.4	0.199	6.66	4.45	0.0089	0.12
1.6	0.268	8.95	8.74	0.0235	0.20
1.7	0.298	9.93	9.97	0.0297	0.23
1.8	0.338	11.27	11.44	0.0387	0.25
1.9	0.370	12.33	14.17	0.0524	0.31
2.1	0.442	14.72	19.00	0.0839	0.44
2.2	0.483	16.10	20.13	0.0972	0.49
2.3	0.527	17.57	30.01	0.1582	0.66
2.4	0.558	18.60	27.60	0.1540	0.60
2.5	0.614	20.47	36.39	0.2235	0.88
2.6	0.654	21.82	31.10	0.2036	0.84
2.7	0.705	23.50	34.78	0.2452	0.83
2.8	0.718	23.84	35.07	0.2519	0.95
2.9	0.773	25.78	44.14	0.3414	1.22
3.1	0.811	27.04	50.55	0.4100	1.42

D: deformation displacement; *J*: $J = 2 U/B b$; Δa : measured crack growth length.

$$J = \int \left(\bar{W} dy - \bar{T} \frac{\partial \bar{U}}{\partial x} ds \right) \quad (1)$$

where the \bar{T} is the surface traction; \bar{W} , the strain energy density; \bar{U} , the displacement vector; and *x* and *y*, the axis coordinates. Rice² and Begley and Landes^{3,4} showed that the *J*-integral can be interpreted as the strain energy change with crack growth, which is expressed as the following:

$$J = - \frac{dU}{Bda} \quad (2)$$

where *B* is the thickness of the loaded body, and *a*, the crack length. *U* is the total strain energy, which can be obtained by measuring the area under the load-displacement curve. Sumpter and Turner later expanded the *J*-integral equation by the following equation³⁶:

$$J = J_e + J_p \quad (3)$$

J_e and *J_p* are the elastic and plastic components of the total *J* value. For a three-point-bend single-edge notched specimen with a span equal to 4*W* and 0.4 < *a/W* < 0.6, eq. (3) can further be expressed by the following equation:

$$J = \frac{2U}{B \cdot (W - a)} \quad (4)$$

ASTM E813 recommends that eq. (4) can be used to calculate the *J* value for an SENB specimen.

The Size Criteria of Specimens

According to ASTM E813 for *J*-testing, a valid *J_{Ic}* value is obtained when the following size criteria is satisfied:

$$B, (W - a), W > 25 \left(\frac{J_c}{\sigma_y} \right) \quad (5)$$

where *B*, *W*, and *W* - *a* are specimen thickness, width, and ligament length, respectively. σ_y is the yield strength. These size criteria produce a plastic plane-strain stress condition at the crack front and allow for the use of significantly smaller specimen dimensions than those required for LEFM testing.

Paris and co-workers³⁷ developed the tearing modulus concept to describe the stability of ductile crack in terms of elastic-plastic fracture mechanics. This fracture instability occurs if the elastic shortening of the system exceeds the corresponding plas-

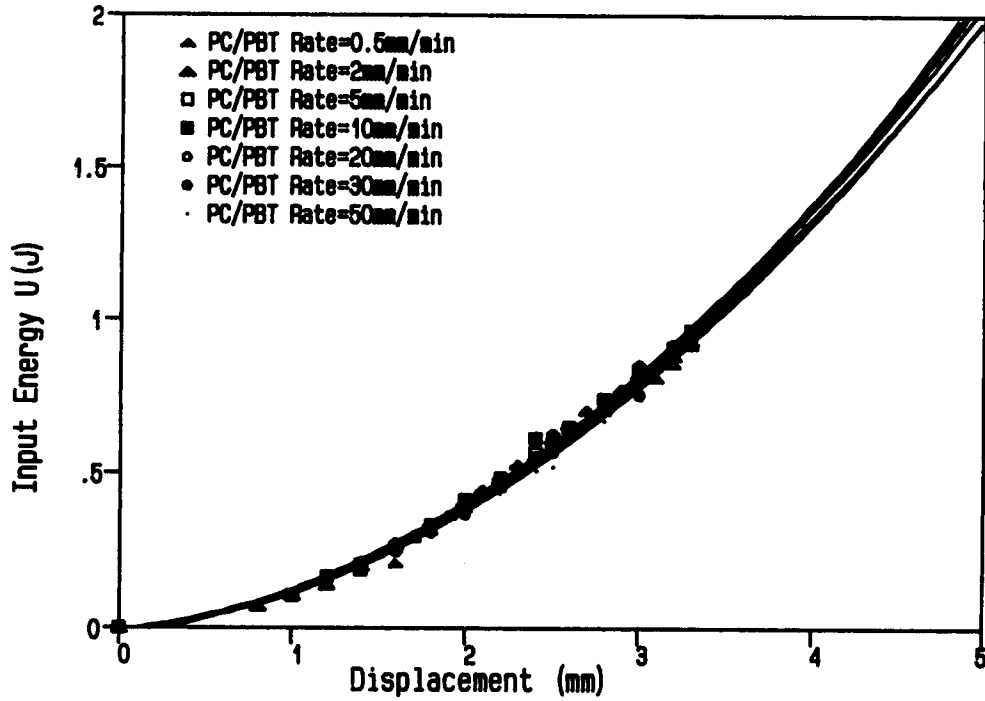


Figure 2 Plots of the input energy vs. displacement at different rates.

tic lengthening for crack extension. A nondimensional parameter, tearing modulus (T_m), has been defined as the following equation³⁷:

$$T_m = \left(\frac{dJ}{da} \right) \cdot \left(\frac{E}{\sigma_y^2} \right) \quad (6)$$

where E and dJ/da are the Young's modulus and the slope of the resistance curve, respectively.

For the $J - \Delta a$ data to be regarded as an intrinsic material property independent of specimen size, the

criterion of $\omega > 10$ must be met according to the following equation:

$$\omega = \frac{(W - a)}{J_c} \cdot \left(\frac{dJ}{da} \right) \quad (7)$$

J-Integral According to Hysteresis Energy Method

There are many practical cases in laboratory tests where it is necessary to evaluate a grossly nonlinear

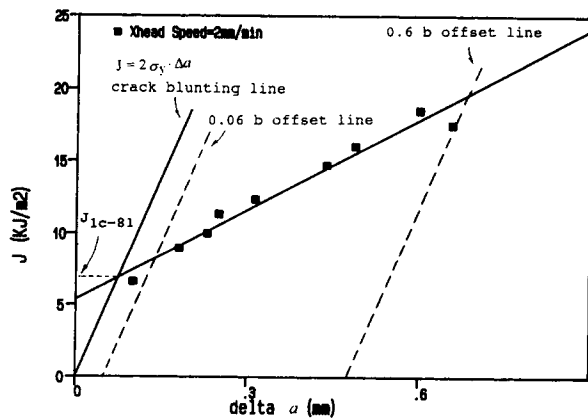


Figure 3 Plot of J vs. Δa according to the ASTM E813-81 method at rate = 2 mm/min.

Table III Critical J_{1c} from ASTM E813 Methods at Different Rates

	Rate (mm/min)						
	0.5	2	5	10	20	30	50
<u>ASTM E813-81 Method</u>							
J_{1c-81} (kJ/m ²)	6.49	7.28	6.91	7.17	7.42	7.08	7.38
J_{0-81} (kJ/m ²)	4.75	5.68	5.08	5.47	5.91	5.45	6.17
<u>ASTM E813-87 Method</u>							
J_{1c-87} (kJ/m ²)	12.37	12.69	12.95	13.41	13.07	13.16	12.62
J_{0-87} (kJ/m ²)	9.19	9.03	9.17	9.79	9.23	10.02	9.47

J_{1c-81} : standard ASTM E813-81 method. J_{0-81} : modified version of ASTM E813-81 method by intercepting $J - \Delta a$ regression line with Y-axis. J_{1c-87} : Standard ASTM E813-87 method. J_{0-87} : modified version of E813-87 by using 0.1 mm offset line.

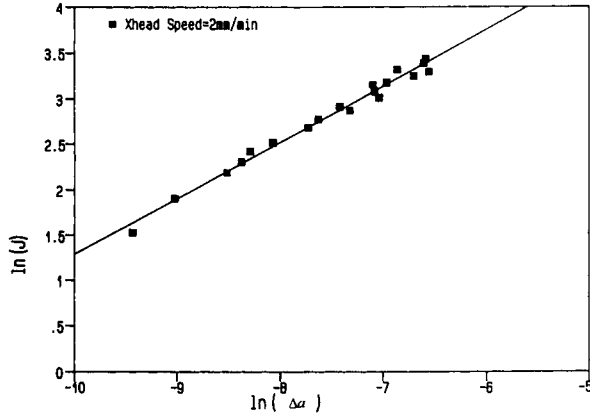


Figure 4 Plot ln J vs. ln Δa at rate = 2 mm/min.

dissipative system. Such a situation was treated by Andrew and Fukahori^{38,39} using a generalized theory. However, this approach requires complicated and time-consuming experiments as well as some assumptions on the nature of the hysteresis behavior. According to Andrew's generalized fracture mechanics theory,^{38,39} the fracture energy of a solid is given by

$$\mathfrak{F} = \mathfrak{F}_0 \cdot \Phi \cdot (\epsilon_0, \dot{a}, T) \tag{8}$$

where \mathfrak{F} is the total fracture energy of the system to cause a unit area of growth; \mathfrak{F}_0 , the energy to rupture the unit area of interatomic bonds across the fracture plane (the "surface energy" of the body); and Φ , a loss function depending on the crack velocity \dot{a} , the temperature, and applied strain ϵ_0 . The loss function is derived as follows:

$$\Phi = \frac{K_1(\epsilon_0)}{\left[K_1(\epsilon_0) - \frac{1}{2} \cdot \sum_{PU} \beta(x, y) \cdot g \cdot \delta_x \cdot \delta_y \right]} \tag{9}$$

where K_1 is a function of strain; x and y , the reduced Cartesian coordinates of point P ; and a , the crack length. $\beta(x, y)$ is the hysteresis ratio at point P , and the symbol PU denotes summation over points which unload as the crack propagates. The evaluation of the term $\sum \beta(x, y) \cdot g \cdot \delta_x \cdot \delta_y$ of eq. (9) requires additional knowledge of the hysteresis ratio β from point to point in the stress field, and β will, in general, be a function of the local strain, strain rate, and temperature. Indeed, β will also, in general, depend on the amount of crack growth, Δa , since the functional energy loss at P will depend on the degree of relaxation permitted to occur there. However, for a steady-state tearing (constant crack speed) as observed in the work reported here, it is appropriate

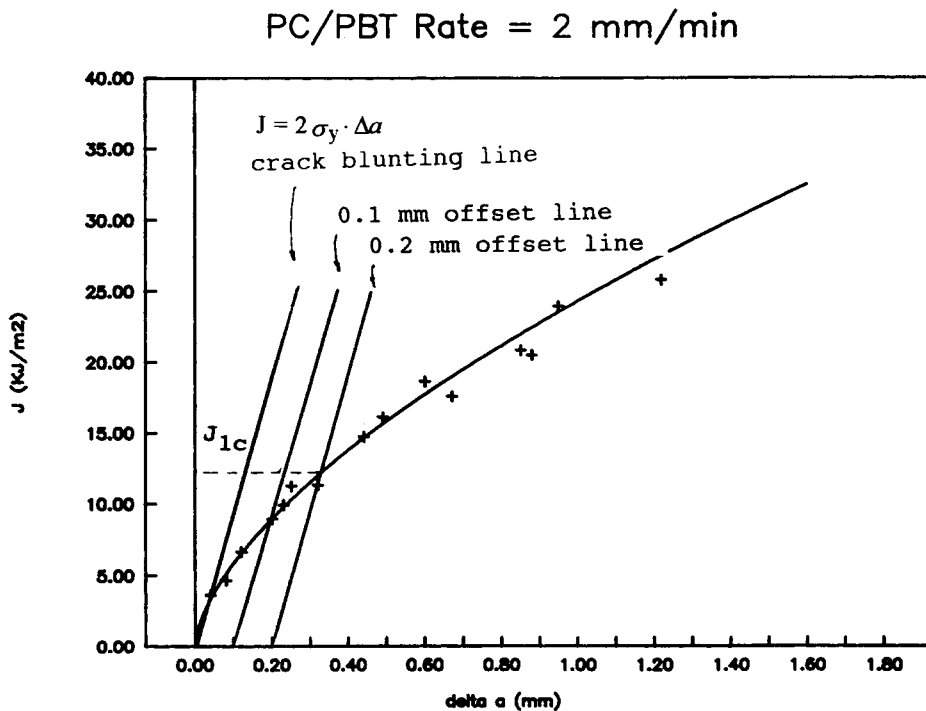


Figure 5 Plot of J vs. Δa according to the ASTM E813-87 method at rate = 2 mm/min.

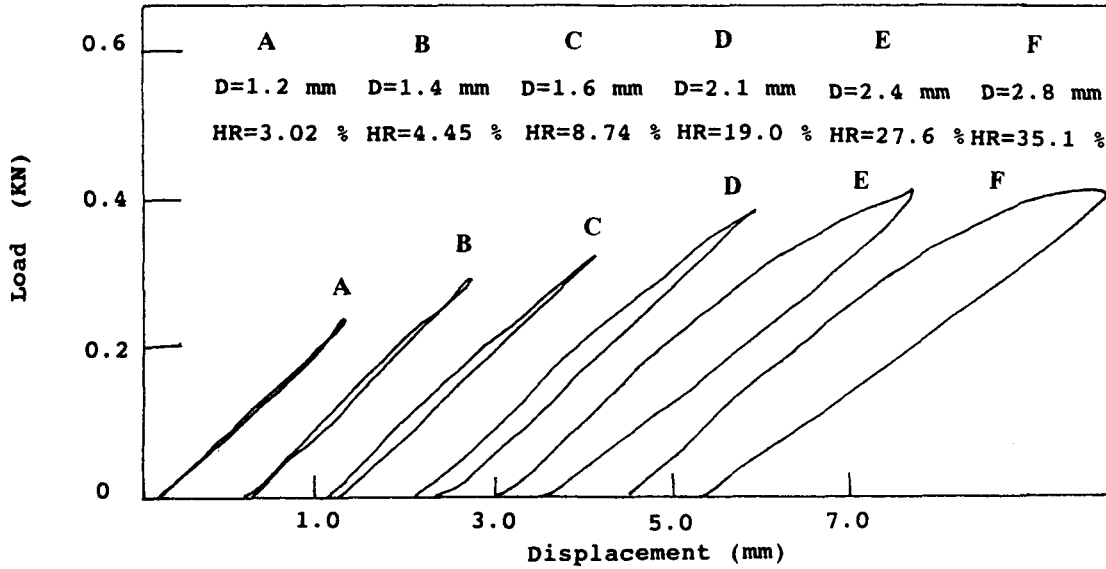


Figure 6 Plot of hysteresis loop at different controlled displacement at rate = 2 mm/min.

to use the hysteresis ratio for a full loading/unloading stress cycle at the appropriate strain rate. We have assumed that the β is a unique function of input energy density at a given strain rate.

The hysteresis ratio defined in this hysteresis energy method is not the same as the one developed by Andrew. It is the energy difference between the input and the recovery in the cyclic loading and unloading steps which may include crack blunting and crack extension stages. The energy density change during crack growth can be presented by the following equation:

$$-\frac{dU}{dA} = a \cdot W_0 \cdot \left[\left(\sum_{PL} g(x, y) \cdot \delta_x \cdot \delta_y \right) - \left(\sum_{PU} G(x, y, \sigma_y) \cdot \delta_x \cdot \delta_y \right) \right] \quad (10)$$

where PL and PU indicate loading and unloading, respectively. W_0 is the input energy density, and g and G are two functions of x, y , and σ_y , respectively. The quantity $-dU/dA$ includes the energy available for forming crack surface and the energy consumed as plastic deformation of the cracked specimen. The input energy density (W_0) can be given by the area (A_0) under the loading curve up to a particular strain ϵ , and the recoverable energy density (W_r) is the area under the unloading covered (A_r). The hysteresis ratio [$HR(\%)$] is then defined by the following equation:

$$HR(\%) = \frac{A_0 - A_r}{A_0} \quad (11)$$

and the hysteresis energy (HE) is then given by

$$HE = HR(\%) \cdot U \quad (12)$$

where U is the input energy at different displacements.

For a cracked specimen, the material surrounding the crack tip can be divided into three parts: $\langle 1 \rangle$, the first plastic zone; $\langle 2 \rangle$, the second plastic zone; and $\langle 3 \rangle$, the elastic fracture surface. The specific

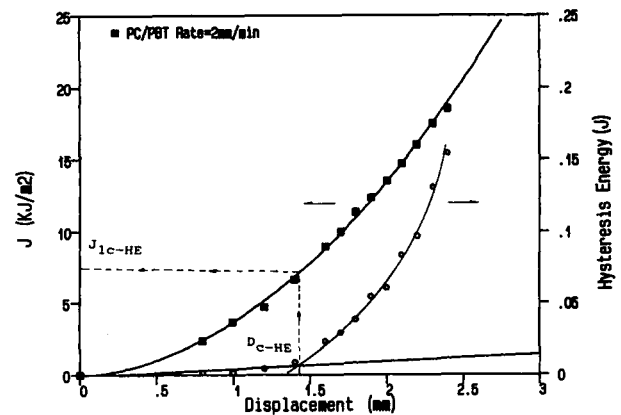


Figure 7 The J_{1c} value determination according to the hysteresis energy method at rate = 2 mm/min.

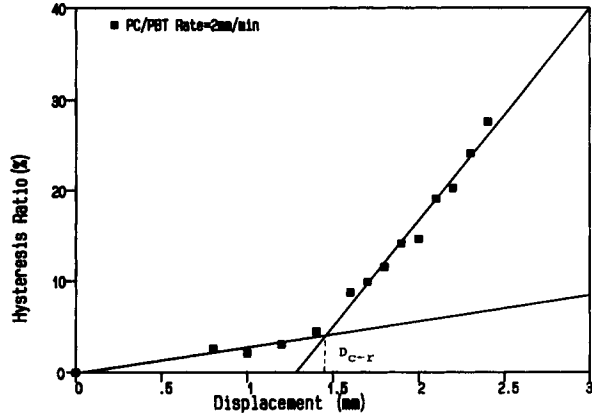


Figure 8 Plot of the hysteresis ratio vs. displacement.

energy balance equation for a cracked specimen can be expressed as the following:

$$\frac{1}{B} \cdot \left(\frac{dU}{da} - \frac{dU_e}{da} - \frac{dU_k}{da} \right) = \frac{1}{B} \cdot \left(\frac{dU_p^{PPZ}}{da} + \frac{dU_p^{SPZ}}{da} \right) + 2\gamma_s \quad (13)$$

and the energy dissipated of the system is given as

$$\frac{dHE}{dA} = \frac{1}{B} \cdot \left(\frac{dU_p^{PPZ}}{da} + \frac{dU_p^{SPZ}}{da} \right) + 2\gamma_s \quad (14)$$

where the U_k is the kinetic energy; U_e , the elastic energy; U_p^{PPZ} , the plastic energy for the primary plastic zone; U_p^{SPZ} , the plastic energy for the secondary plastic zone; and γ_s , the fracture surface energy. In our previous articles,⁴⁰⁻⁴³ the relation between the precrack hysteresis and the corresponding ductile-brittle transition behavior of polycarbonate and polyacetal has been reported. When a precrack specimen is under loading before the onset of crack extension (during blunting), a significant portion of the input energy is consumed and converted into a relatively larger crack tip plastic zone for the toughened polymers. These viscoelastic and inelastic energies may include many possible energy dissipated micromechanisms such as crazing, cavitation, debonding, and shear yielding which can be related to the measured hysteresis energy. The hysteresis energy will increase gradually with the increase of load from the load vs. displacement curve. After crack extension, the strain energy release due to crack growth will be added into the observed total hysteresis energy. The rate of the hysteresis energy increase due to this strain energy release is signifi-

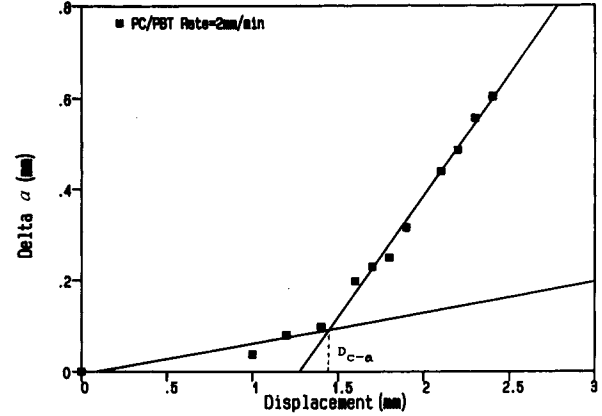


Figure 9 Plot of the crack growth length vs. displacement.

cantly higher than those above-mentioned precrack micromechanisms. Therefore, in a plot of hysteresis energy vs. deformation displacement of a notched specimen, a clear transition from crack blunting to crack extension can be identified. Such a phenomenon, a drastic increase of the hysteresis energy immediately after the onset of crack extension, can be used to determine the critical fracture toughness (J_{1c}) as the onset of crack extension. The data observed to support this viewpoint were presented in our previous articles.³⁰⁻³⁵

EXPERIMENTAL

The PC/PBT blend (Alotex C701) was obtained from Alotex Polymer Alloy Corp. of Taiwan. Injection-molded PC/PBT specimens with dimensions of $20 \times 90 \times 8$ mm were prepared by an Arbury injection-molding machine. All specimens were sharpened with a fresh razor blade. All the notched

Table IV Critical Displacement D_c and Critical J_{1c} from the Hysteresis Energy Method at Different Rates

	Rate						
	0.5	2	5	10	20	30	50
D_{c-HE} (mm)	1.51	1.42	1.49	1.48	1.51	1.47	1.48
J_{1c-HE} (kJ/m ²)	7.65	7.47	7.95	7.79	7.80	7.16	7.53
D_{c-a} (mm)	1.53	1.46	1.51	1.51	1.49	1.53	1.54
D_{c-r} (mm)	1.52	1.47	1.50	1.49	1.56	1.69	1.79

D_c : critical initial displacement. HE : from the plot of hysteresis energy vs. displacement by using the power law propagation line. a : from the plot of the measured crack growth length vs. displacement. r : from the plot of hysteresis ratio vs. displacement.

Table V The Size Criterion Requirements for Valid J_{1c} of ASTM E813 Methods at Different Rates

	Rate (mm/min)						
	0.5	2	5	10	20	30	50
ASTM E813-81 Method							
dJ/da	20.71	19.46	19.71	21.16	20.59	21.61	16.62
$25(J_{1c-81})/\sigma_y$	3.63	3.91	3.69	3.78	3.71	3.48	3.52
T_m	19.12	17.21	19.66	21.27	20.23	23.29	18.53
ω parameter	31.91	26.73	28.52	29.51	27.74	30.52	22.52
$\omega > 10$	Yes	Yes	Yes	Yes	Yes	Yes	Yes
Plane strain	Yes	Yes	Yes	Yes	Yes	Yes	Yes
ASTM E813-87 Method							
dJ/da	26.25	27.75	27.85	28.85	29.44	28.72	25.64
$25(J_{1c-87})/\sigma_y$	6.93	6.82	6.93	7.07	6.54	6.46	6.02
T_m	24.23	24.54	27.78	29.01	28.93	30.96	28.58
ω parameter	21.22	21.86	21.51	21.51	22.52	21.82	20.31
$\omega > 10$	Yes	Yes	Yes	Yes	Yes	Yes	Yes
Plane strain	Yes	Yes	Yes	Yes	Yes	Yes	Yes

$$T_m = E/\sigma_y^2 \cdot dJ/da. \quad \omega = (W - a)/J_{1c} \cdot dJ/da.$$

specimens were annealed at 60°C for 2 h to release the residual stress prior to the standard three-point bend testing. The J -integral testing was carried out according to the multiple-specimen method outlined in ASTM E813-81 at ambient condition and at a series testing strain rate from 0.5 to 50 mm/min with the span to width ratio of 4. The crack growth length was measured at the center of the fracture surface by freezing the deformed specimens in liquid nitrogen, then breaking them with a pendulum impact tester. Hysteresis tests were carried out by loading at a predetermined displacement, then unloading at the same strain rate. Tensile tests were performed according to the ASTM D638 standard with different strain rates (range from 0.5 to 50 mm/min).

RESULTS AND DISCUSSION

Table I summarizes the yield strength σ_y and Young's modulus E at strain rates varying from 0.5 to 50 mm/min; both σ_y and E increase with increase of the strain rate.

J_{1c} Determination by ASTM Standards and Modified Versions

The complete fracture load-displacement curves of the PC/PBT blend at different rates are shown in

Figure 1. The multiple-specimen technique used to load the specimen to a controlled displacement on the curve and then unload following the ASTM method. The J value for each specimen at each controlled displacement is calculated by using eq. (4), and the corresponding crack growth length, Δa , is measured from the surface of the broken specimen. Detailed data for the specimen with $B = 8$ mm and rate = 2 mm/min are summarized in Table II. Figure 2 shows the plots of the input energy vs. displacement at different rates, which are generally independent of the test rate ranging from 0.5 to 50 mm/min. Figure 3 shows the plot of the acceptable J vs. Δa by a linear regression line according to the ASTM E813-81 method. This linear regression intercepts with the blunting line to locate the critical J_{1c-81} value. The J_{1c-81} values obtained from the E813-81 method are generally independent of the crosshead speed range used in this investigation. Another critical J_{1c} value (J_{o-81}) is determined at the interception of the linear regression resistance curve with the Y-axis as recommended by Narisawa and Takemori¹⁶; the obtained J_{o-81} is slightly lower (20–30%) than that from the E813-81 method due to the neglect of the crack blunting phenomenon of the crack tip. All these data from ASTM E813-81 and its modified methods at different rates are summarized in Table III.

In the ASTM E813-87 method, the values of the C_1 and C_2 of the power regression line, $J = C_1(\Delta a)C_2$,

are obtained from the plot of $\ln J$ vs. $\ln \Delta a$ within the exclusion lines between $\Delta a = 0.15$ and 1.5 mm as shown in Figure 4. The obtained power law of $J = C_1(\Delta a)C_2$ at different rates gives the following equations:

For rate = 0.5 mm/min,

$$J = 1173(\Delta a)^{0.569}$$

For rate = 2 mm/min,

$$J = 1723(\Delta a)^{0.617}$$

For rate = 5 mm/min,

$$J = 1694(\Delta a)^{0.614}$$

For rate = 10 mm/min,

$$J = 1519(\Delta a)^{0.593}$$

For rate = 20 mm/min,

$$J = 2028(\Delta a)^{0.632}$$

For rate = 30 mm/min,

$$J = 1396(\Delta a)^{0.580}$$

For rate = 50 mm/min,

$$J = 907(\Delta a)^{0.534}$$

The J_{1c} is then located at the intercept between the power law fit line and the 0.2 mm offset line as shown in Figure 5 at rate = 2 mm/min. The data obtained from the ASTM E813-87 method are summarized in Table III. The J_{1c} values obtained from the E813-817 method are about 60–80% higher than those from the corresponding E813-81 method. Only very limited comparative J_{1c} data between the two ASTM standards (E813-81 and E813-87) on polymeric materials have been previously reported. Huang¹⁸ recently reported that the J_{1c} from the E813-87 method of the rubber-toughened nylon 6, 6 is significantly higher than that from E813-81 method (38 vs. 15 kJ/m²). We also found that the J_{1c} values obtained from the E813-87 method for the elastomer-modified polycarbonate³⁰ and high-impact polystyrene³² are also about 20–40% higher than those from the E813-81 method. If the 0.2 mm offset line specified in E813-87 is now revised to 0.1

mm and the rest of the procedure remains unchanged as shown in Figure 5, the resultant J_{1c} obtained now becomes comparable to that from the E813-81 method (Table III). Similar results were also obtained from the elastomer-modified polycarbonate,³⁰ the high-impact polystyrene,³² and the polycarbonate/acrylonitrile-butadiene-styrene.³⁵

J_{1c} Determination by the Hysteresis Method

Figure 6 illustrates the hysteresis loops and their corresponding hysteresis ratio at various stages of displacement at the rate = 2 mm/min. The hysteresis ratio and energy of each specimen at different displacements are calculated by eqs. (11) and (12), respectively. The results of the hysteresis ratio and hysteresis energy at different displacements are summarized in Table II. The experimentally measured hysteresis energy is believed to be higher than the true hysteresis energy because of the time-dependent nature of the polymers. It is impossible to obtain the true hysteresis energy at the endpoint of loading. However, for steady-state tearing (constant crack speed) as observed in this study, it is appropriate to use the hysteresis ratio for a fully loading/unloading stress cycle at the appropriate deform rate. Figure 7 combines the plots of the hysteresis energy and J vs. crosshead displacement at a rate equal to 2 mm/min. The crack initiation displacement (D_c) is located at the intersection between the blunting line and the second order polynomial regression propagation line. As soon as the D_c is located, the J_{1c-HE} is then determined from the plot of the J vs. the displacement curve. Since the measurement of crack growth length is no longer necessary by this hysteresis energy method, it is easier than are the ASTM E813 methods. The J_{1c-HE} values obtained from the hysteresis energy method are close to the E813-81 method, but still lower than the E813-87 method, as shown in Table III.

Figure 8 shows the plots of hysteresis ratio vs. crosshead displacement of the PC/PBT blend at a rate = 2 mm/min. The critical displacement, intersection of the bilinear lines, is assumed as the displacement due to the onset of crack initiation. The critical initiation displacements lie between 1.4 and 1.5 mm for a rate varying from 0.5 to 50 mm/min. The plotting of the crosshead displacement vs. crack growth length at a rate = 2 mm/min is shown in Figure 9; the critical displacement is now located at the intersection between two linear regression lines. The critical displacements obtained are also lie between 1.4 and 1.5 mm for a rate varying from 0.5 to

50 mm/min. The critical displacements from these three methods, hysteresis energy vs. displacement, hysteresis ratio vs. displacement, and crack growth length vs. displacement, are fairly close. That means that the critical displacement from hysteresis methods (energy or ratio) is, indeed, as is the displacement, due to the onset of crack extension. Table IV summarizes these three critical D_c and J_{c-HE} values of the PC/PBT blend at different rates by this hysteresis energy method.

The Size Criterion of Specimens

According to ASTM E813 for J -testing, a valid J_{1c} value is obtained when the B , $(W - a)$, $W > 25 (J_{1c}/\sigma_y)$ size criterion has been satisfied. These size criteria produce a plastic plane-strain stress condition at the crack front and allow for the use of significantly smaller specimen dimensions than those required for LEFM testing. Table V shows that the size criteria are met for the specimen with $B = 8$ mm at different rates. A nondimensional parameter, tearing modulus (T_m), has been defined as eq. (6). The dJ/da values obtained according to the linear regression R -curves of ASTM E813-81 and dJ/da values obtained according to the power law regression curve of ASTM E813-87 at $\Delta a = 0.2$ mm at different rates are summarized in Table V. These results indicate that the dJ/da values obtained from the E813-87 method are about 40–50% higher than from the E813-81 method; however, both dJ/da values are independent of the test rates, varying from 0.5 to 50 mm/min. For the $J - \Delta a$ data to be regarded as an intrinsic material property independent of specimen size, the criterion of $\omega > 10$ must be met. In this study, the specimen dimensions employed meet the ASTM size criterion ($\omega > 10$) as shown in Table V.

CONCLUSION

This hysteresis energy method is able to inherently adjust for the occurrence of the crack blunting and thus avoids the controversy of the blunting issue. Besides, it is simple without the requirement of the tedious crack growth length measurements. The J_{1c} values obtained from the hysteresis energy method are comparable with those from the E813-81 method but are about 60–80% lower than those from the E813-87 method. J_{1c} values determined from the ASTM E813-81, E813-87, and hysteresis energy methods are independent of the test rate. The B ,

$(W - a)$, $W > 25 (J_{1c}/\sigma_y)$ size criterion requirements of ASTM E813 and the $\omega > 10$ criterion are all satisfied in this study.

The authors are grateful to the National Science Council of Republic of China for financial support.

REFERENCES

1. ASTM Standard E399-78, in *Annual Book of ASTM Standards*, 1978, Part 10, p. 540.
2. J. R. Rice, *J. Appl. Mech.*, **35**, 379 (1968).
3. J. A. Begley and J. D. Landes, *ASTM STP*, **514**, 1 (1972).
4. J. D. Landes and J. A. Begley, *ASTM STP*, **560**, 170 (1974).
5. M. K. V. Chan and J. G. Williams, *Int. J. Fract.*, **19**, 145 (1983).
6. M. K. V. Chan and J. G. Williams, *Polym. Eng. Sci.*, **21**, 1019 (1981).
7. S. Hashemi and J. G. Williams, *Polymer*, **27**, 85 (1986).
8. D. D. Huang and J. G. Williams, *J. Mater. Sci.*, **22**, 2503 (1987).
9. P. K. So and L. J. Broutman, *Polym. Eng. Sci.*, **26**, 1173 (1986).
10. E. J. Moskala and M. R. Tant, *Polym. Mater. Sci. Eng.*, **63**, 63 (1990).
11. C. M. Rimnac, T. M. Wright, and R. W. Klein, *Polym. Eng. Sci.*, **28**, 1586 (1988).
12. I. Narisawa, *Polym. Eng. Sci.*, **27**, 41 (1987).
13. D. S. Parker, H. J. Sue, J. Huang, and A. F. Yee, *Polymer*, **31**, 2267 (1990).
14. N. Haddaoui, A. Chudnovsky, and A. Moet, *Polymer*, **27**, 1337 (1986).
15. I. C. Tung, *Polym. Bull.*, **25**, 253 (1991).
16. I. Narisawa, and M. T. Takemori, *Polym. Eng. Sci.*, **29**, 671 (1989).
17. D. D. Huang and J. G. Williams, *Polym. Eng. Sci.*, **30**, 1341 (1990).
18. D. D. Huang, *Polym. Mater. Sci. Eng.*, **63**, 578 (1990).
19. B. S. Westerlind, L. A. Carlsson, and Y. M. Andersson, *J. Mater. Sci.*, **26**, 2630 (1991).
20. J. R. Rice, P. C. Paris, and J. G. Merkle, *ASTM STP*, **536**, 231 (1973).
21. S. N. Afluri, M. Ankagami, and W. H. Chen, *ASTM STP*, **631**, 42 (1977).
22. C. F. Shin, M. D. Germann, and V. Kumar, *J. Pressure Vessel Piping*, **9**, 159 (1981).
23. ASTM Standard E813-81, in *Annual Book of ASTM Standards*, 1981, Part 10, p. 810.
24. ASTM Standard E813-87, in *Annual Book of ASTM Standards*, 1987, Part 10, p. 968.
25. S. Seidler and W. Grellmann, *J. Mater. Sci.*, **28**, 4078 (1993).

26. Y. W. Mai and B. Cotterell, *J. Mater. Sci.*, **15**, 2296 (1980).
27. Y. W. Mai and B. Cotterell, *Eng. Fract. Mech.*, **21**, 123 (1985).
28. J. Wu, Y. W. Mai, and B. Cotterell, *J. Mater. Sci.*, **28**, 3373 (1993).
29. W. N. Chung and J. G. Williams, *ASTM STP*, **1114**, 320 (1991).
30. C. B. Lee and F. C. Chang, *Polym. Eng. Sci.*, **32**, 792 (1992).
31. C. B. Lee, M. L. Lu, and F. C. Chang, *J. Chin. Inst. Chem. Eng.*, **23**, 305 (1992).
32. C. B. Lee, M. L. Lu, and F. C. Chang, *Polym. Eng. Sci.*, to appear.
33. C. B. Lee, M. L. Lu, and F. C. Chang, *J. Appl. Polym. Sci.*, **47**, 1867 (1993).
34. M. L. Lu, C. B. Lee, and F. C. Chang, *J. Mater. Sci.*, to appear.
35. M. L. Lu, C. B. Lee, and F. C. Chang, *Polymer*, to appear.
36. J. D. Sumpter and C. E. Turner, *Int. J. Fract.*, **9**, 320 (1973).
37. P. C. Paris, H. Tada, A. Zahoor, and H. Ernst, *ASTM STP*, **668**, 5 (1979).
38. E. H. Andrews, *J. Mater. Sci.*, **9**, 887 (1974).
39. E. H. Andrews and Y. Fukahori, *J. Mater. Sci.*, **12**, 1307 (1977).
40. F. C. Chang and H. C. Hsu, *J. Appl. Polym. Sci.*, **43**, 1025 (1991).
41. F. C. Chang and M. Y. Yang, *Polym. Eng. Sci.*, **30**, 543 (1990).
42. F. C. Chang and H. C. Hsu, *J. Appl. Polym. Sci.*, **47**, 2195 (1993).
43. F. C. Chang and H. C. Hsu, *J. Appl. Polym. Sci.*, **52**, 1981 (1994).

Received August 20, 1994

Accepted November 13, 1994